



Contents lists available at ScienceDirect

Bioorganic & Medicinal Chemistry Letters

journal homepage: www.elsevier.com/locate/bmcl

Lobeline analogues containing 4-hydroxy and 4-(2-fluoroethoxy) aromatic substituents: Potent and selective inhibitors of [³H]dopamine uptake at the vesicular monoamine transporter-2



Shyamsunder R. Joolakanti^{a,†}, Justin R. Nickell^{b,†}, Venumadhav Janganati^a, Guangrong Zheng^a, Linda P. Dwoskin^b, Peter A. Crooks^{a,*}

^a Department of Pharmaceutical Sciences, College of Pharmacy, University of Arkansas for Medical Sciences, Little Rock, AR 72205, USA

^b Department of Pharmaceutical Sciences, College of Pharmacy, University of Kentucky, Lexington, KY 40536, USA

ARTICLE INFO

Article history:

Received 10 March 2016

Revised 30 March 2016

Accepted 31 March 2016

Available online 1 April 2016

Keywords:

4-Hydroxyphenyl lobeline analogues

Fluorinated lobeline analogues

Vesicular monoamine transporter-2

Dopamine uptake

Dopamine and serotonin transporter

ABSTRACT

A series of lobeline and GZ-793A analogues that incorporate aromatic 4-hydroxy and 4-(2-fluoroethoxy) substituents were synthesized and evaluated for inhibition of [³H]dopamine (DA) uptake at the vesicular monoamine transporter-2 (VMAT2) and the dopamine transporter (DAT), and [³H]serotonin uptake at the serotonin transporter (SERT). Most of these compounds exhibited potent inhibition of DA uptake at VMAT2 in the nanomolar range ($K_i = 30\text{--}70\text{ nM}$). The two most potent analogues, **7** and **14**, both exhibited a K_i value of 31 nM for inhibition of VMAT2. The lobeline analogue **14**, incorporating 4-(2-fluoroethoxy) and 4-hydroxy aromatic substituents, exhibited 96- and 335-fold greater selectivity for VMAT2 versus DAT and SERT, respectively, in comparison to lobeline. Thus, lobeline analogues bearing hydroxyl and fluoroethoxy moieties retain the high affinity for VMAT2 of the parent compound, while enhancing selectivity for VMAT2 versus the plasmalemma transporters.

© 2016 Elsevier Ltd. All rights reserved.

Methamphetamine (METH) abuse is a serious burden on the United States, with approximately 100,000 new METH users every year.¹ METH abuse constitutes significant health risks, such as long term neuronal damage, psychosis, paranoia, insomnia, anxiety, aggression, delusions, and hallucinations, and chronic use ultimately may lead to death.² Currently, there are no FDA-approved medications to treat METH addiction. METH users describe a sudden rush of pleasure lasting for several minutes to hours upon self-administration of the drug. These reinforcing properties of METH result from METH-induced prolonged release of dopamine (DA) into the extracellular space, where it interacts with postsynaptic DA receptors.³ METH enters dopaminergic presynaptic terminals via passive diffusion through the plasmalemma membrane, and as a substrate for the plasmalemma DA transporter (DAT).⁴ Once inside the terminal, METH evokes the release of vesicular DA from synaptic vesicles into the cytosol through an interaction with the vesicular monoamine transporter-2 (VMAT2).⁴ Since METH also inhibits the activity of the mitochondrial enzyme, monoamine oxidase (MAO), the METH-evoked increase in cytosolic DA is not subjected to metabolism,

and the formation of dihydroxyphenylacetic acid (DOPAC).⁵ The increase in cytosolic DA concentrations makes DA more readily available for release into the extracellular compartment via reversal of DAT. The resulting release of DA from the presynaptic terminal, and the subsequent enhanced stimulation of postsynaptic DA receptors results in the reinforcing effects and the high abuse liability associated with METH.⁶ In this respect, heterologous VMAT2 knockout mice exhibit reduced amphetamine conditioned reward, enhanced amphetamine locomotion, and enhanced sensitivity to amphetamine, clearly indicating the importance of VMAT2 in mediating the behavioral effects of this related psychostimulant.⁷

Lobeline is the principal alkaloid of the Indian tobacco plant, *Lobelia inflata*. Lobeline inhibits DA uptake into synaptic vesicles via an interaction with the tetrabenazine (TBZ) binding site on VMAT2, but does not inhibit MAO activity.⁸ Lobeline attenuates METH self-administration in a rodent model, but importantly, does not substitute for METH in the self-administration paradigm, indicating that it lacks abuse liability.⁹ Lobeline also decreases METH-induced hyperactivity and behavioral sensitization in rats.⁹ Also, lobeline decreases METH-evoked DA release from superfused rat striatal slices, while concurrently increasing extracellular DOPAC.^{8a} Based on these preclinical findings, lobeline was considered a lead candidate as a treatment for METH abuse. Unfortunately, lobeline also acts as a nicotinic acetylcholine receptor antagonist.¹⁰ Drugs

* Corresponding author. Tel.: +1 501 686 6495; fax: +1 501 686 6057.

E-mail address: paccrooks@uams.edu (P.A. Crooks).

[†] These authors contributed equally to this manuscript and are co-first authors.

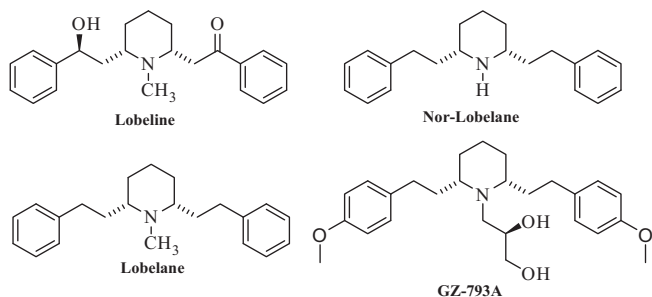


Figure 1. Chemical structure of lobeline, lobelane, nor-lobelane, GZ-793A. Lobeline is the principal alkaloid of *Lobelia inflata*. Lobelane is a chemically defunctionalized, saturated derivative of lobeline. GZ-793A is a 4-methoxy analogue of nor-lobelane incorporating an *N*-(2*S*)-1,2-dihydroxypropyl substituent.

which exhibit such neurochemical profiles have the potential to generate untoward side-effects in the clinical population. To overcome these limitations, several structure–activity relationship (SAR) studies were performed which involved modifying the chemical structure of lobeline, and assessing the influence of these structural alterations on selectivity of the novel compounds for VMAT2 versus nicotinic receptors and plasmalemma neurotransmitter transporters, DAT and the serotonin transporter (SERT).¹⁰

Lobelane is a structurally modified derivative of lobeline (Fig. 1), which exhibits 10- to 15-fold higher potency for inhibiting VMAT2 function compared to lobeline.¹¹ Importantly, structural defunctionalization of lobeline to afford lobelane markedly diminished nicotinic receptor affinity of lobelane and associated analogues. Lobelane also inhibits METH-evoked DA release from rat striatal slice preparations.¹¹ To improve upon the physicochemical properties of lobelane, we synthesized a lobelane analogue, GZ-793A, by structural modification of the *N*-methyl group in the molecule to an *N*-(2*S*)-1,2-dihydroxypropyl moiety (Fig. 1). This structural

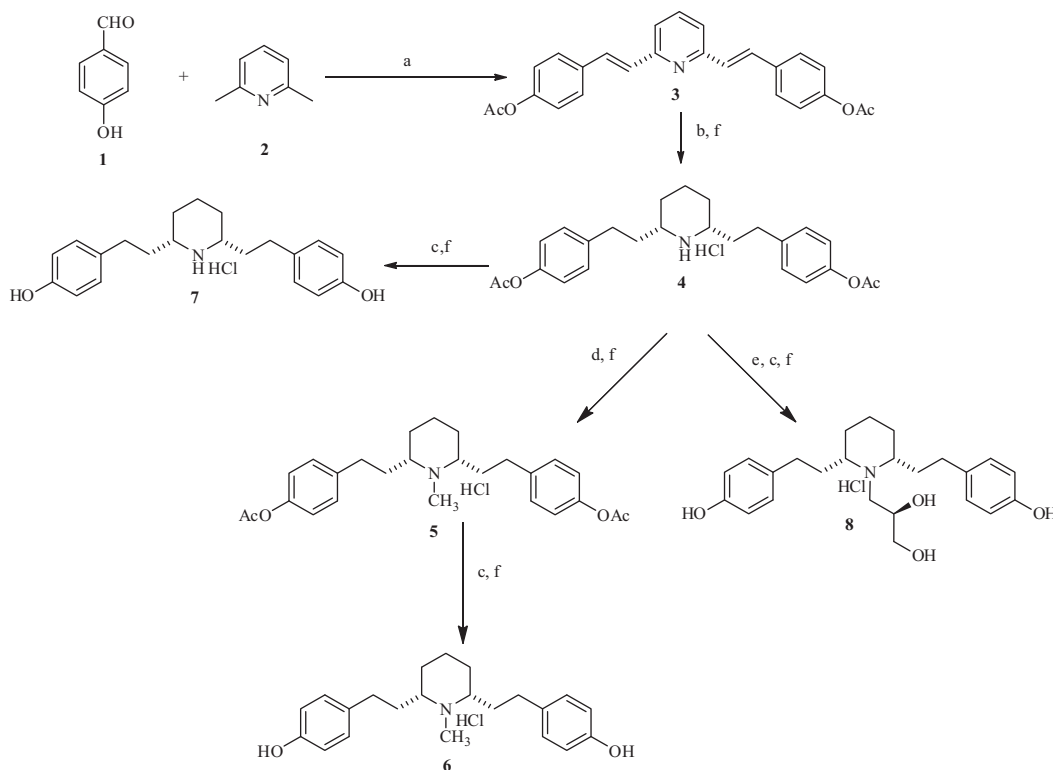
modification significantly improved affinity for VMAT2 and drug-likeness properties.¹² Notably, this compound blocked METH self-administration in rats, but had no effect on responding for food.¹³

In the present study, we report on the synthesis of several new lobelane derivatives that incorporate novel functional groups onto the phenyl rings of lobelane and GZ-793A.

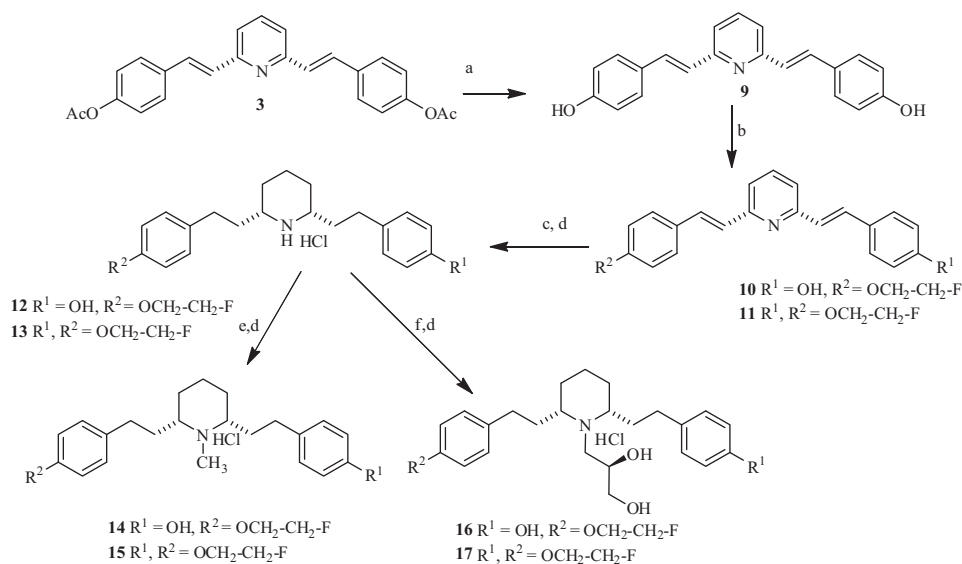
Moreover, several of the synthesized compounds were fluorine-containing analogues and are of potential value in positron emission tomography (PET) studies when prepared incorporating the ¹⁸F positron-emitting isotope (half-life ~120 min). The incorporation of fluorine into the structure of a drug molecule also influences lipophilic, electronic, and metabolic properties, all of which can critically influence both the pharmacodynamic and pharmacokinetic properties of the drug.¹⁴

The synthesis of the lobelane and GZ-793A derivatives utilized compound **3** as a starting point (Scheme 1). Compound **3** was synthesized by the reaction of 4-hydroxybenzaldehyde (**1**) with 2,6-lutidine (**2**) in acetic anhydride at reflux temperature. Intermediate, **3** was subjected to hydrogenation using Adams catalyst (PtO₂) in acetic acid to yield a saturated piperidino derivative, which was further converted to hydrochloride salt **4** using HCl in diethyl ether. Compound **4** was reacted with NaBH₃CN/HCHO to obtain *N*-methylated compound **5**. Compounds **4** and **5** were de-acetylated in presence of K₂CO₃ in MeOH and followed by hydrochloride salt formation to afford the corresponding free hydroxyl compounds **6** and **7**, respectively. Compound **4** was reacted with *S*-glycidol in ethanol, followed by de-acetylation in presence of K₂CO₃ in MeOH and formation of hydrochloride salt to obtain the *N*-(2*S*)-1,2-dihydroxypropyl derivative **8** (Scheme 1).

The fluorine-containing derivatives of lobelane and GZ-793A were synthesized from intermediate **3**. Compound **3** was de-acetylated in the presence of K₂CO₃ in MeOH to afford **9**, which was *O*-alkylated utilizing ethylfluorotrylate and sodium hydroxide in DCM/MeOH (2:1) to yield a mixture of monofluoroethoxy



Scheme 1. Reagents and conditions: (a) Ac₂O, reflux, 24 h, 48%; (b) 10% (w/v) PtO₂/H₂, AcOH, 12 h, 65%; (c) K₂CO₃/MeOH, rt, 1 h, 90–95%; (d) HCHO/NaBH₃CN, EtOH, 2 h, 61%; (e) *S*-glycidol, EtOH, reflux, 2 h, 57–60%; (f) 2 M HCl in ether.



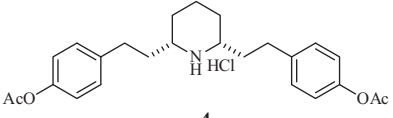
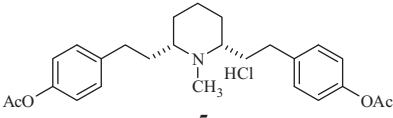
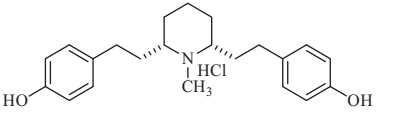
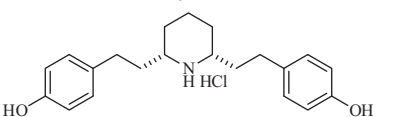
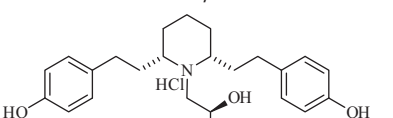
Scheme 2. Reagents and conditions: (a) K₂CO₃/MeOH, rt, 1 h; (b) F-CH₂-CH₂-OTs, NaOH, DCM/MeOH (2:1), 2 h, 30–33%; (c) 10% (w/v) PtO₂/H₂, AcOH, 12 h, 60–65%; (d) DCM/2 M HCl in ether; (e) HCHO/NaBH₃CN, EtOH, 2 h 58–61%; (f) (S)-glycidol, EtOH, reflux, 2 h, 57–60%.

derivative **10** and difluoroethoxy derivative **11** (Scheme 2). After careful separation of these two compounds by silica gel column chromatography, **10** and **11** were each hydrogenated using Adams catalyst (PtO₂) in acetic acid to yield the corresponding saturated piperidino derivatives, which were further converted to their hydrochloride salts to obtain **12** and **13**, respectively. Compounds **12** and **13** were then treated with NaBH₃CN/HCHO to obtain the

N-methylated derivatives **14** and **15**. N-(2S)-1,2-Dihydroxypropyl derivatives **16** and **17** were obtained by reacting **12** and **13** with S-glycidol in ethanol (Scheme 2). The synthesized compounds were fully characterized by ¹H NMR, ¹³C NMR and high resolution mass spectral analysis.

Compounds **4–8** and **12–17** were evaluated initially for inhibition of VMAT2 function (Tables 1 and 2; Fig. 2). The majority of

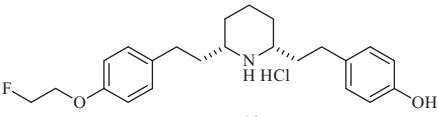
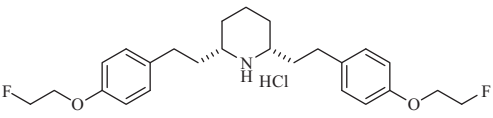
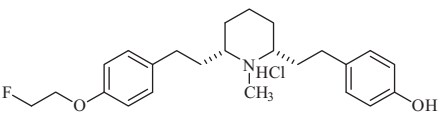
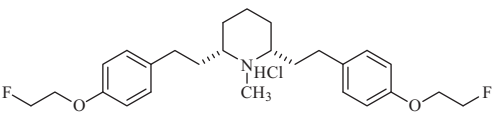
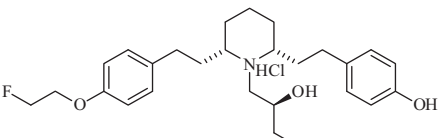
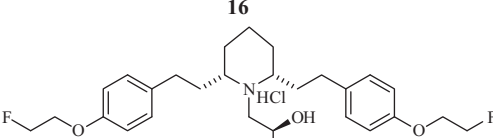
Table 1
Inhibition of [³H]DA uptake at VMAT2 and DAT, and inhibition of [³H]5-HT uptake at SERT by precursor non-fluorinated lobelane analogues

Compound	VMAT2 [³ H]DA Uptake (K _i ; μM)	DAT [³ H]DA Uptake (K _i ; μM)	SERT [³ H]5-HT Uptake (K _i ; μM)
Lobelane	0.067 ± 0.007 ^b	1.05 ± 0.03 ^b	3.6 ± 0.35 ^b
GZ-793A	0.029 ± 0.008 ^b	1.44 ± 0.27 ^b	9.36 ± 2.74 ^b
	0.22 ± 0.021 ^a	1.47 ± 0.403	2.13 ± 0.466
	0.071 ± 0.008	2.13 ± 0.87	11.6 ± 1.46
	0.046 ± 0.005	1.35 ± 0.34	12.0 ± 2.00
	0.031 ± 0.004	0.866 ± 0.14	1.03 ± 0.17
	0.039 ± 0.003	1.43 ± 0.73	12.9 ± 2.98

^a Data represent mean ± SEM (n = 3–4 rats/analogue).

^b Data taken from Ref. 15 (Horton et al., 2011).

Table 2Inhibition of [³H]DA uptake at VMAT2 and DAT, and inhibition of [³H]5-HT uptake at SERT by fluorinated lobelane analogues

Compound	VMAT2 [³ H]DA Uptake (K_i ; μM)	DAT [³ H]DA Uptake (K_i ; μM)	SERT [³ H]5-HT Uptake (K_i ; μM)
Lobelane	0.067 ± 0.007^b	1.05 ± 0.03^b	3.6 ± 0.35^b
GZ-793A	0.029 ± 0.008^b	1.44 ± 0.27^b	9.36 ± 2.74^b
 12	0.032 ± 0.003^a	1.66 ± 0.34	1.05 ± 0.29
 13	0.040 ± 0.002	1.67 ± 0.30	0.640 ± 0.034
 14	0.031 ± 0.003	2.97 ± 0.46	10.4 ± 0.54
 15	0.14 ± 0.011	3.43 ± 0.73	7.43 ± 1.84
 16	0.063 ± 0.003	5.47 ± 0.92	1.43 ± 0.23
 17	0.120 ± 0.003	3.69 ± 0.72	33.0 ± 2.92

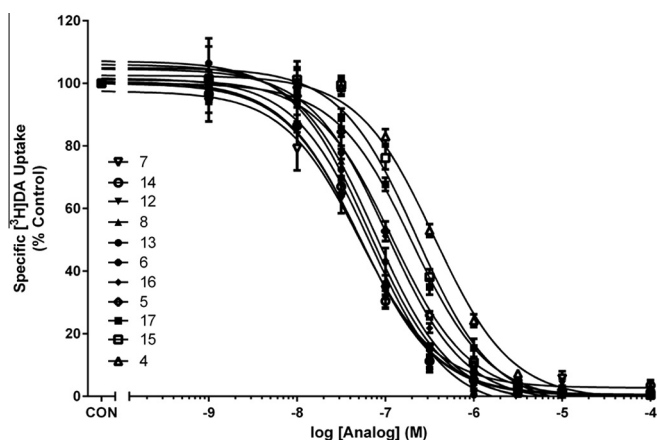
^a Data represent mean \pm SEM ($n = 3\text{--}4$ rats/analogue).^b Data taken from Ref. 15 (Horton et al., 2011).

Figure 2. Lobelane and GZ-793A analogues inhibit [³H]DA uptake at VMAT2 in rat striatal vesicles. Concentration–response curves for inhibition of VMAT2. Order of presentation for the analogues within the figure legend is from high to low affinity for VMAT2. Control (CON) represents [³H]DA uptake in the absence of compound. Data are mean (\pm SEM) specific [³H]DA uptake expressed as a percentage of control (24.8 ± 1.06 pmol/min/mg, control $n = 42$ rats; $n = 3\text{--}4$ rats/compound).

the compounds exhibited affinities for VMAT2 within a relatively restricted range of 30–70 nM. Incorporation of 4-acetoxy substituents into the phenyl rings of nor-lobelane afforded **4**, which exhibited a K_i value of 0.22 μM in the VMAT2 assay. N-methylation of **4** afforded **5**, which had threefold improved inhibitory potency at VMAT2 ($K_i = 0.071$ μM). Hydrolysis of the 4-acetoxy groups in **4** and **5** gave the diphenolic analogues **7** and **6**, respectively, with about twofold further improvement in inhibitory potency at VMAT2 ($K_i = 0.031$ μM and 0.046, respectively). These data indicate that introduction of aromatic hydroxyl substituents into the lobelane molecule retains the high inhibitory potency at VMAT2 exhibited by lobelane. Interestingly, this trend was also observed for compound **8**, a diphenolic analogue of GZ-793A, which exhibited K_i of 0.039 μM in the VMAT2 assay (Table 1).

Evaluation of nor-lobelane analogues **12** and **13**, the mono-4-(2-fluoroethoxy) and di-4-(2-fluoroethoxy) derivatives of **7**, indicated that replacing the phenolic groups in these compounds with 2-fluoroethoxy groups had little effect on inhibition of DA uptake at VMAT2 (K_i 's = 0.032 and 0.040, respectively) in relation to analogue **7**. N-methylation of **12** afforded compound **14**, one of the most potent inhibitors ($K_i = 0.031$ μM) of vesicular DA uptake in the series. However, while the di-4-(2-fluoroethoxy) analogue **13** afforded a K_i value of 0.040 μM , which is not different from that of lobelane or GZ-793A, insertion of either a *N*-methyl group

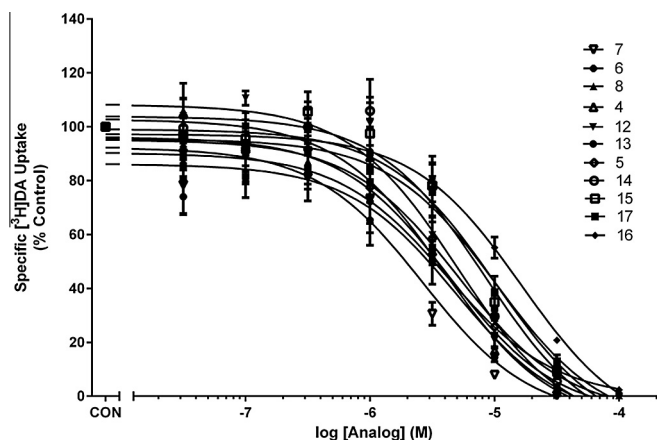


Figure 3. Lobelane and GZ-793A analogues inhibit [³H]DA uptake at DAT in rat striatal synaptosomes. Concentration–response curves for inhibition of DAT. Order of presentation for the analogues within the figure legend is from high to low affinity for DAT. Control (CON) represents [³H]DA uptake in the absence of compound. Data are mean (±SEM) specific [³H]DA uptake expressed as a percentage of control (19.5 ± 1.27 pmol/min/mg, control *n* = 43 rats; *n* = 3–4 rats/compound).

(compound **15**, $K_i = 0.14 \mu\text{M}$) or a *N*-(2*S*)-1,2-dihydroxypropyl group (compound **17**, $K_i = 0.120 \mu\text{M}$) in place of the piperidino hydrogen atom in **13** reduces potency at VMAT2 by 3–3.5-fold. It is important to note that compound **16**, a mono-4-(2-fluoroethoxy) analogue of GZ-793A, exhibited a K_i value of 0.063 μM in the VMAT2 assay, and represents a lead fluorine-containing analogue with improved water solubility over lobelane.

Potency of VMAT2 inhibition alone is insufficient to determine whether the discovery of these novel lobelane analogues have clinical potential as treatments for METH abuse. Accordingly, we also examined the ability of these compounds to inhibit the plasmalemma transporters, DAT and SERT (Tables 1 and 2; Figs. 3 and 4). Generally, all of the analogues in this study exhibited affinities for DAT comparable to those for both lobelane ($K_i = 1.05 \mu\text{M}$) and GZ-793A ($K_i = 1.44 \mu\text{M}$).¹⁵ Likewise, a preponderance of the compounds inhibited SERT with affinities not different from those for lobelane ($K_i = 3.6 \mu\text{M}$) and GZ-793A ($K_i = 9.36 \mu\text{M}$).¹⁵ Notable exceptions to these generalizations are compound **13** which has sixfold greater affinity for SERT than lobelane, compound **16** which has a sevenfold greater affinity for SERT than GZ-793A, and compound **17** which exhibits a fourfold decrease in affinity for SERT when compared to GZ-793A. Thus, compound **17** exhibits 30- and 275-fold greater selectivity for VMAT2 versus DAT and SERT, respectively. While incorporation of 2-fluoroethoxy moieties into the structural scaffold of GZ-793A does not alter affinity for VMAT2 in comparison to both lobelane ($K_i = 67 \text{ nM}$) and GZ-793A ($K_i = 29 \text{ nM}$), the greater selectivity for VMAT2 exhibited by these compounds suggests a low likelihood of abuse liability.¹⁵

Similar to lobelane and GZ-793A, all the compounds evaluated in this study exhibited higher affinities for VMAT2 than DAT and SERT. Most compounds showed 15 to 40-fold greater selectivity for VMAT2 versus the plasmalemma transporters. The combination of 4-(2-fluoroethoxy) and 4-hydroxy aromatic substitution present in compounds **14** and **16** afforded the greatest selectivity for VMAT2 versus DAT, 96- and 87-fold respectively. Lobelane analogue **14** was one of the most potent VMAT inhibitors in the series. Likewise, incorporation of 4-acetoxy and 4-hydroxy aromatic substituents into the phenyl rings of lobelane resulted in improvement in selectivity for VMAT2 versus SERT; compounds **5**, **6** and **8** exhibited selectivity ratios of 163, 260- and 331-fold, respectively. Overall, compound **14** demonstrated 96- and 335-fold selectivity for VMAT2 versus DAT and SERT, respectively, and was the most selective analogue of the series.

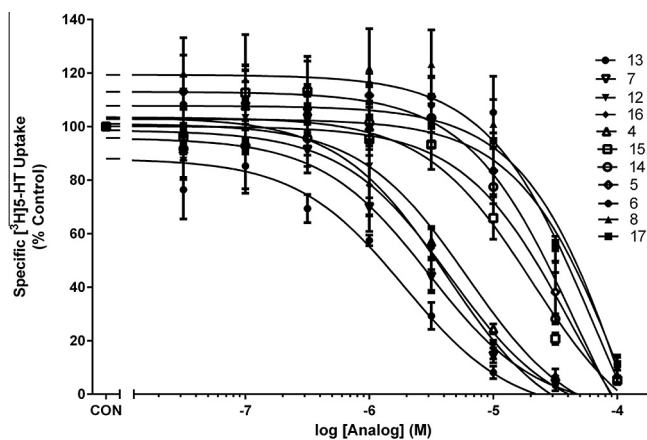


Figure 4. Lobelane and GZ-793A analogues inhibit [³H]5-HT uptake at SERT in rat striatal synaptosomes. Concentration–response curves for inhibition of SERT. Order of presentation for the analogues within the figure legend is from high to low affinity for SERT. Control (CON) represents [³H]5-HT uptake in the absence of compound. Data are mean (±SEM) specific [³H]5-HT uptake expressed as a percentage of control (4.46 ± 0.234 pmol/min/mg, control *n* = 44 rats; *n* = 4 rats/compound).

In summary, a series of lobelane and GZ-793A analogues that incorporate aromatic 4-hydroxy and aromatic 4-(2-fluoroethoxy) substituents were synthesized and evaluated for their ability to inhibit [³H]DA uptake at VMAT2 and DAT, and [³H]5-HT uptake at SERT.¹⁶ Incorporation of these moieties into the structure of lobelane generally maintained inhibitory potency at VMAT2 relative to the parent compound. The potent VMAT2 inhibitor **14**, which incorporates 4-(2-fluoroethoxy) and 4-hydroxy aromatic substituents, exhibited the greatest selectivity for VMAT2 versus DAT and SERT. These results also indicate that fluorinated lobelane and GZ-793A analogues retain the high inhibitory potency and selectivity of lobelane and GZ-793A for VMAT2, and as such constitute promising candidates for the visualization of VMAT2 via PET scanning in the clinical population.

Acknowledgements

This research was supported by NIH U01 DA13519, 5T32 DA022981, TR000117 and NIH/COBRA P20 GM109005 grants, and an Arkansas Research Alliance (ARA) Scholar award.

Supplementary data

Supplementary data associated with this article can be found, in the online version, at <http://dx.doi.org/10.1016/j.bmcl.2016.03.119>.

References and notes

- Substance Abuse and Mental Health Services Administration, Office of Applied Studies, 2008.
- Nordahl, T. E.; Salo, R.; Leamon, M. J. *Neuropsychiatry Clin. Neurosci.* **2003**, *15*, 317.
- Pifl, C.; Drobny, H.; Hornykiewicz, O.; Singer, E. A. *Mol. Pharmacol.* **1995**, *47*, 368.
- Johnson, R. A.; Eshleman, A. J.; Meyers, T.; Neve, K. A.; Janowsky, A. *Synapse* **1998**, *30*, 97.
- Mantle, T. J.; Tipton, K. F.; Garrett, N. J. *Biochem. Pharmacol.* **1976**, *25*, 2073.
- (a) Fisher, J. F.; Cho, A. K. *J. Pharmacol. Exp. Ther.* **1979**, *208*, 203; (b) Liang, N. Y.; Rutledge, C. O. *Biochem. Pharmacol.* **1982**, *31*, 983; (c) Ary, T. E.; Komiskey, H. L. *Life Sci.* **1980**, *26*, 575; (d) Sulzer, D.; Chen, T. K.; Lau, Y. Y.; Kristensen, H.; Rayport, S.; Ewing, A. *J. Neurosci.* **1995**, *15*, 4102.
- (a) Takahashi, N.; Miner, L. L.; Sora, I.; Ujike, H.; Revay, R. S.; Kostic, V. *Proc. Natl. Acad. Sci. U.S.A.* **1997**, *94*, 9938; (b) Wang, Y.; Gainetdinov, R. R.; Fumagalli, F.; Xu, F.; Jones, S. R.; Book, C. B. *Neuron* **1997**, *19*, 1285.
- (a) Teng, L. H.; Crooks, P. A.; Dwoskin, L. P. *J. Pharmacol. Exp. Ther.* **1997**, *280*, 1432; (b) Teng, L. H.; Crooks, P. A.; Sonsalla, P. K.; Dwoskin, L. P. *J. Neurochem.*

- 1998, 71, 258; (c) Nickell, J. R.; Krishnamurthy, S.; Norrholm, S.; Deaciuc, A. G.; Siripurapu, K. B.; Zheng, G.; Crooks, P. A.; Dwoskin, L. P. *J. Pharmacol. Exp. Ther.* **2010**, 332, 612.
9. (a) Harrod, H. B.; Dwoskin, L. P.; Crooks, P. A.; Klebaur, J. E.; Bardo, M. T. *J. Pharmacol. Exp. Ther.* **2001**, 298, 172; (b) Harrod, H. B.; Dwoskin, L. P.; Green, T. A.; Gehrke, B. J.; Bardo, M. T. *Psychopharmacology* **2003**, 387, 97.
 10. (a) Miller, D. K.; Crooks, P. A.; Dwoskin, L. P. *Neuropharmacology* **2000**, 39, 2654; (b) Miller, D. K.; Crooks, P. A.; Zheng, G.; Grinevich, V. P.; Norrholm, S. D.; Dwoskin, L. P. *J. Pharmacol. Exp. Ther.* **2004**, 310, 1035.
 11. (a) Zheng, G.; Dwoskin, L. P.; Deaciuc, A. G.; Norrholm, S. D.; Crooks, P. A. *J. Med. Chem.* **2005**, 48, 5551; (b) Vartak, A. P.; Nickell, J. R.; Chagkutip, J.; Dwoskin, L. P.; Crooks, P. A. *J. Med. Chem.* **2009**, 52, 7878; (c) Vartak, A. P.; Deaciuc, A. G.; Dwoskin, L. P.; Crooks, P. A. *Bioorg. Med. Chem. Lett.* **2010**, 20, 3584.
 12. (a) Crooks, P. A.; Zheng, G.; Vartak, A. P.; Culver, J. P.; Zheng, F.; Horton, D. B.; Dwoskin, L. P. *Curr. Top. Med. Chem.* **2011**, 11, 1103; (b) Zheng, G.; Dwoskin, L. P.; Deaciuc, A. G.; Zhu, J.; Jones, M. D.; Crooks, P. A. *Bioorg. Med. Chem.* **2005**, 13, 3899; (c) Zheng, G.; Dwoskin, L. P.; Deaciuc, A. G.; Crooks, P. A. *Bioorg. Med. Chem. Lett.* **2005**, 15, 4463; (d) Zheng, G.; Dwoskin, L. P.; Deaciuc, A. G.; Crooks, P. A. *Bioorg. Med. Chem. Lett.* **2008**, 18, 6509.
 13. (a) Alvers, K. M.; Beckmann, J. S.; Zheng, G.; Crooks, P. A.; Dwoskin, L. P.; Bardo, M. T. *Psychopharmacology (Berl.)* **2012**, 224, 255; (b) Beckmann, J. S.; Denehy, E. D.; Zheng, G.; Crooks, P. A.; Dwoskin, L. P.; Bardo, M. T. *Psychopharmacology (Berl.)* **2012**, 220, 395.
 14. Elliott, A. J.; Hudlicky, M.; Pavlath, A. E. *ACS Monograph* **1995**, 187, 1119.
 15. Horton, D. B.; Siripurapu, K. B.; Zheng, G.; Crooks, P. A.; Dwoskin, L. P. *J. Pharmacol. Exp. Ther.* **2011**, 339, 286.
 16. **Vesicular [³H]DA Uptake Assay.** Inhibition of [³H]DA uptake was conducted as previously described,^{8b} utilizing a striatal synaptic vesicle preparation. Briefly, rat striata were homogenized with 10 up and down strokes of a Teflon pestle homogenizer (clearance ~0.003") in 14 mL of 0.32 M sucrose solution. Homogenates were centrifuged (2000g for 10 min at 4 °C), and the resulting supernatants were centrifuged again (10,000g for 30 min at 4 °C). Pellets were resuspended in 2 ml of 0.32 M sucrose solution and subjected to osmotic shock by adding 7 mL of ice-cold water to the preparation, followed by the immediate restoration of osmolality by adding 900 µL of 0.25 M HEPES buffer and 900 µL of 1.0 M potassium tartrate solution. Samples were centrifuged (20,000g for 20 min at 4 °C), and the resulting supernatants were centrifuged again (55,000g for 1 h at 4 °C), followed by addition of 100 µL of 10 mM MgSO₄, 100 µL of 0.25 M HEPES and 100 µL of 1.0 M potassium tartrate solution prior to the final centrifugation (100,000g for 45 min at 4 °C). Final pellets were resuspended in 2.4 mL of assay buffer (25 mM HEPES, 100 mM potassium tartrate, 50 µM EGTA, 100 µM EDTA, 1.7 mM ascorbic acid, 2 mM ATP-Mg²⁺, pH 7.4). Aliquots of the vesicular suspension (100 µL) were added to tubes containing assay buffer, various concentrations of analogue inhibitor (0.1 nM–10 mM) and 0.1 µM [³H]DA in a final volume of 500 µL. Nonspecific uptake was determined in the presence of Ro4-1284 (10 µM). Reactions were terminated by filtration, and radioactivity retained by the filters was determined by liquid scintillation spectrometry (Liquid scintillation analyzer; PerkinElmer Life and Analytical Sciences, Boston, MA).
- Synaptosomal [³H]DA and [³H]5-HT Uptake Assays.** Analogue-induced inhibition of [³H]DA and [³H]5-HT uptake into rat striatal synaptosomes, was determined using modifications of a previously described method.¹⁵ Striata were homogenized in 20 ml of ice-cold 0.32 M sucrose solution containing 5 mM NaHCO₃, pH 7.4, with 16 up-and-down strokes of a Teflon pestle homogenizer (clearance ~0.005 inch). Homogenates were centrifuged at 2000g for 10 min at 4 °C, and resulting supernatants were centrifuged at 20,000g for 17 min at 4 °C. Pellets were re-suspended in 1.5 mL of Krebs' buffer, containing 125 mM NaCl, 5 mM KCl, 1.5 mM MgSO₄, 1.25 mM CaCl₂, 1.5 mM KH₂PO₄, 10 mM α-D-glucose, 25 mM HEPES, and 0.1 mM EDTA, with 0.1 mM pargyline and 0.1 mM ascorbic acid, saturated with 95% O₂/5% CO₂, pH 7.4. Synaptosomal suspensions (20 µg of protein/50 µL) were added to duplicate tubes containing 50 µL of analogue (7–9 concentrations; 0.1 nM–1 mM, final concentration) and 350 µL of buffer and incubated at 34 °C for 5 min in a total volume of 450 µL. Samples were placed on ice, and 50 µL of [³H]DA or [³H]5-HT (10 nM, final concentration) was added to each tube for a final volume of 500 µL. Reactions proceeded for 10 min at 34 °C and were terminated by the addition of 3 mL of ice-cold Krebs' buffer. Nonspecific [³H]DA and [³H]5-HT uptake were determined in the presence of 10 µM GBR 12909 and 10 µM fluoxetine, respectively. Samples were rapidly filtered through Whatman (Clifton, NJ) GF/B filters using a cell harvester (MP-43RS; Brandel Inc., Gaithersburg, MD). Filters were washed three times with 4 mL of ice-cold Krebs' buffer containing catechol (1 mM). Complete counting cocktail was added to the filters, and radioactivity was determined by liquid scintillation spectrometry (B1600 TR scintillation counter; PerkinElmer Life and Analytical Sciences